Journal of Catalysis 282 (2011) 74–82

Contents lists available at ScienceDirect

Journal of Catalysis

journal homepage: www.elsevier.com/locate/jcat

C–H bond activation of methane on clean and oxygen pre-covered metals: A systematic theoretical study

Bin Xing [a], Xian-Yong Pang [b], Gui-Chang Wang [a,*]

[a] Department of Chemistry, Nankai University, Tianjin 300071, PR China
[b] College of Chemistry and Chemical Engineering, Taiyuan University of Technology, Taiyuan 030024, PR China

ARTICLE INFO

Article history:
Received 25 February 2011
Revised 19 May 2011
Accepted 30 May 2011
Available online 20 July 2011

Keywords:
Methane activation
Metal
Oxygen
Reactive trends
Density functional calculation

ABSTRACT

Density functional theory calculations are presented for adsorption and dissociation of CH_4 on clean and oxygen atom pre-adsorbed metal surfaces (Cu, Ag, Au, Ni, Pd, Pt, Ru, Rh, Os, Ir, and Mo). The total energy change and the activation barrier have been calculated for the direct and the oxygen-assisted cleavage of the C–H bonds. Our results indicate that pre-adsorbed oxygen promotes the CH_4 dissociation process on IB group metal surfaces, but inhibits the dissociation process on transition metal surfaces. A good Brønsted–Evans–Polanyi correlation for CH_4 dissociation on clean and atomic oxygen pre-adsorbed metal surfaces is found, which is helpful to reveal the nature of CH_4 dissociation. From the analysis of activation barrier, we expect our work can provide a clear understanding of the nature of CH_4 dissociation.

© 2011 Elsevier Inc. All rights reserved.

1. Introduction

CH_4 is a low-cost material that could provide energy by hydrogen extraction or as a basis species for the synthesis of more sophisticated molecules [1]. So, the dissociation process has led to a number of experimental and theoretical studies. For complex real-world catalytic process, surface modifiers offer an important and challenging area of research for industry and economy. In recent decades, much work has been performed to investigate the effect of the pre-adsorbed atomic oxygen on the activity of the metal surface both experimentally and theoretically [2–15]. It is of considerable interest in connection with a number of crucial technological processes such as bulk oxidation, corrosion, and heterogeneous catalysis [16]. For example, oxygen strongly activates the oxygen–, carbon–, sulfur–, and nitrogen–hydrogen bonds on noble metal surfaces, but also inhibits their dissociation on more active metals [4–9]. Wise et al. studied the reaction of CH_4 with pre-adsorbed oxygen atom on Ni(1 0 0) and Ni(1 1 1) [11,12]. They found that the activity for CH_4 reaction was significantly increased by the presence of oxygen. Alstrup et al. reported that there is no evidence for oxygen-enhanced dissociation of CH_4 on Ni(1 0 0) [13], and they did find a significant increase in reactivity for CH_4 dissociation on O/Cu(1 0 0) [14]. Valden et al. examined CH_4 dissociative chemisorption on Pt(1 1 1), and the results indicated that CH_4 dissociation was poisoned by oxygen due to a steric hinderance of active adsorption sites [15]. Au et al. reported that oxygen at hollow sites promoted CH_4 dissociation on Pt, Cu, Ag, and Au, but showed no such effect on the other transition metals [17]. From the comprehensive reviews on CH_4 dissociation [10–15,17,18], one can infer that, depending on the specific metal surface, this dissociation process can either be promoted or be deactivated.

In this study, effect of pre-adsorbed atomic oxygen on the activity of sequential CH_4 dissociation steps on different metal surfaces (Cu, Ag, Au, Ni, Pd, Pt, Rh, Ru, Os, Ir, and Mo) is analyzed. We also want to answer the following questions: what is the general trend for the catalytic activity of the sequential CH_4 dissociation steps on these metals? Is the catalyst poisoned and how is the dissociation process affected by the pre-adsorbed atomic oxygen? Our paper is organized as follows. In Section 2, we introduce the details of calculation methods and the models. In Section 3, the results and analysis of energy decomposition are discussed. Then, we conclude by discussing the effect of oxygen atom on the activation barrier in Section 4.

2. Calculation methods and models

To study the energy and structure details of CH_4 dissociation, the periodic, self-consistent density functional theory (DFT) calculation was performed by using the Vienna ab initio simulation package (VASP) [19–21]. The electronic structures were calculated using DFT within GGA-PW91 [22–24]. The projector augmented wave (PAW) [23,24] scheme was used to describe the inner cores,

* Corresponding author. Fax: +86 22 23502458.
E-mail address: wangguichang@nankai.edu.cn (G.-C. Wang).

0021-9517/$ - see front matter © 2011 Elsevier Inc. All rights reserved.
doi:10.1016/j.jcat.2011.05.027

and the electronic states were expended in a plane wave basis with kinetic cutoff energy of 400 eV. The transition state (TS) was located by three steps: The general NEB method was employed to find an approximated TS, then the quasi-Newton algorithm was used to optimize the likely TS until the force acting on the atom is smaller than 0.03 eV/Å, and last the frequency analysis was carried out to confirm the TS. Activation energy (E_a) and reaction energy (ΔH) were related to the stable molecule in the gas phase.

The surface was modeled by a periodic slab containing four atomic layers with full relaxation of the uppermost two layers. The $p(2 \times 2)$ unit cell was used in this study, which means the coverage of adsorbates and pre-adsorbed oxygen atom is 1/4 monolayer (ML). The Monkhorst–Pack meshes of $4 \times 4 \times 1$special k-point sampling in the surface Brillouinzone were used [25]. A large k-point of $9 \times 9 \times 1$ was chosen during the calculation of electronic structures for accurate results. The optimized lattice constant of 3.64, 4.18, 4.18, 3.53, 3.96, 3.99, 2.74, 3.82, 2.75, 3.86, and 3.15 Å is used for these transition metal surfaces (Cu, Ag, Au, Ni, Pd, Pt, Ru, Rh, Os, Ir, and Mo).

Different calculation parameters such as PBE functional, number of layers, vacuum size, and k-point sampling were considered to select the most reasonable ones. The reaction barriers of CH_4 dissociation on Ni, Cu, and Au surface have been verified with PBE functional. The energy difference is 0.09, 0.01, and 0.01 eV for CH_4 dissociation on Ni, Cu, and Au with different functional. Adsorption system of CH_3 on Ni surface is chosen to study the influence of other parameters (number of layers (4 and 6 layers), the vacuum size (from 10 to 15 Å), and k-point sampling ($4 \times 4 \times 1$, $5 \times 5 \times 1$ and $6 \times 6 \times 1$)). It is found that the adsorption energy difference is less than 0.02 eV with different parameters.

3. Results and discussion

3.1. Adsorption properties of possible species

In order to find out how CH_4 dissociation is affected by the existence of an oxygen atom, the sequential change $CH_4 \overset{(O)}{\rightarrow} CH_3 \overset{(O)}{\rightarrow} CH_2 \overset{(O)}{\rightarrow} CH \overset{(O)}{\rightarrow} CH$, from the free CH_4 molecule to adsorbed C atom is considered on all these transition metal surfaces. The effect of dissociated H atom is not considered in our calculations, and H adsorption on O/Ni(1 0 0) surface[18] at 1/4 ML oxygen coverage ends in hydroxyl formation, a result which is introduced in the present work. The reaction mechanism can be described as $CH_x \rightarrow CH_{x-1} + H$ (x = 1–4) and $CH_x + O \rightarrow CH_{x-1} + H(O)$ (x = 1–4).

In order to investigate the energy profile of CH_4 dissociation on different transition metal surfaces, it is necessary to confirm that adsorption and co-adsorption are favorable at specific site for all possible species involved. The possible species are CH_4, CH_3, CH_2, CH, C, H, O, OH and combination of two of these species. Fig. 1a–d shows the calculated adsorption energies of different species on different transition metal surfaces with and without pre-adsorbed oxygen (also see the Table S1 in the supporting information). For a particular species, all metals in the series seem to have the same stable adsorb site or of similar nature. For example, CH_4 physically adsorbs at the top site [18], the preferred bonding sites of CH_3 vary among the metals, that is, bridge site or the top site [17,18].

It is interesting to analyze the relative stability of CH_x species on different metal surfaces. As seen in Fig. 1, it is clear that the adsorption energies of CH_x species tend to increase with decreasing number of H atom. Being chemically relevant and consistent with the bond order conservation principle, it is in good agreement with the linear correlation found by Abild-Pedersen et al. [26] for the adsorption energies of any CH_x (x = 1–4) species with the adsorption of C atom on transition metal surfaces ('scaling relationship'). That is $E_{ads}^{CH_x} = \gamma(x)E_{ads}^{C} + \xi$ where E_{ads}^{C} is the adsorption energy of atomic C, $E_{ads}^{CH_x}$ is the adsorption energy of CH_x (x = 1–4) species, and ξ and γ are the correlation parameters, corresponding to different adsorbates. Fig. 1e and f shows adsorption energies of CH_x (x = 1–3) plotted against adsorption energies of C for the most stable adsorption sites on both clean surfaces and oxygen pre-adsorbed surfaces. For CH_x (x = 1–3) adsorption on clean surfaces, the slope of the straight line, γ is given to an approximation by $\gamma(x) = \frac{x_{max} - x}{x_{max}}$. Here, x_{max} is the number of H atoms that can bond to C, that is $x_{max} = 4$. $x_{max} - x$ means the valency of CH_x molecule, it can be concluded that the slope only depends on the valency of CH_x molecule. The C atom of CH, CH_2, and CH_3 species is unsaturated, which has a strong tendency to recover its missing bonds. Via formation of C–M bond with surface metal atoms, each unsaturated sp^3 hybrid of C atom binds independently to the d-states of the nearest neighbor metal atoms, that is, CH prefers the hollow site, CH_2 prefers the bridge or hollow site, and CH_3 prefers the top or bridge site. This rule is not suitable for the O/M surface, though there is a nearly linear relationship between $E_{ads}^{CH_x}$ and E_{ads}^{C} (Fig. 1f). The possible reason is that the existence of the oxygen atom changes the charge distribution of the surface and also affects the bonding competition between the oxygen atom and CH_x group. Abild-Pedersen et al., who investigated the nature of this interaction, reported to be independent of the metal [26], so it can be obtained from calculations on any metal surface. In this paper, we analyzed the relationship between adsorption energies of C atom on Cu in order to obtain the value of ξ, which is used to estimate adsorption energies of CH_x on other metal surfaces. The value of ξ was found to be 0.08, -0.18 and -1.11 for CH_3, CH_2, and CH, respectively. Then, we compared the estimated data with the calculated results, which is shown in Fig. 1e (see the dashed line). It is found that these two linear relationships are almost the same; thus, this method can be used to correlate the adsorption energies of CH_x on different metal surfaces.

3.2. CH_4 dissociation on clean and oxygen pre-adsorbed metal surfaces

The activation of the C–H bond occurs via a similar mechanism on clean and O/M surfaces. It can occur by stretching it over the top of metal atom on the surface or through a valley between metal atoms. CH_4 activation occurs over the top of a metal atom. In contrast, CH_3, CH_2, and CH activation processes occur through the valley between metal atoms. The calculated activation (E_a) and reaction energy (ΔH) are shown in Fig. 2 as well as Tables S2–6 in the supporting information.

3.2.1. CH_4 dissociation on the clean metal surface

In the present work, we first analyze the first dissociation step of CH_4, that is, $CH_4 \rightarrow CH_3 + H$. CH_4 activation requires cleavage of a σ-CH bond only interacting with a single metal atom. The reaction path does not vary when the surface is altered. From the total energies shown in Fig. 2, one can see that on the IB group metals, the dissociation step is rather endothermic. The large positive reaction heat corresponds to higher activation barrier, which is at least about 1 eV higher than other transition metal surfaces. On Ni, Ru, Pt, the dissociation step is nearly thermoneutral; on Pd, Rh, Os, Ir, it is slightly endothermic or exothermic, and it is exothermic with a value of -0.45 eV on Mo. The activation barrier on these transition metal surfaces is not very different from each other, and it is in the range between 0.39 eV and 0.69 eV. This is in good agreement with previous results reported by other workers [17,27–30]. It is noteworthy that the small adsorption energy of CH_4 on metal surface does not affect the calculated activation barrier. It was known that the DFT calculation usually underestimates the binding energy of weakly adsorbed molecular like methane

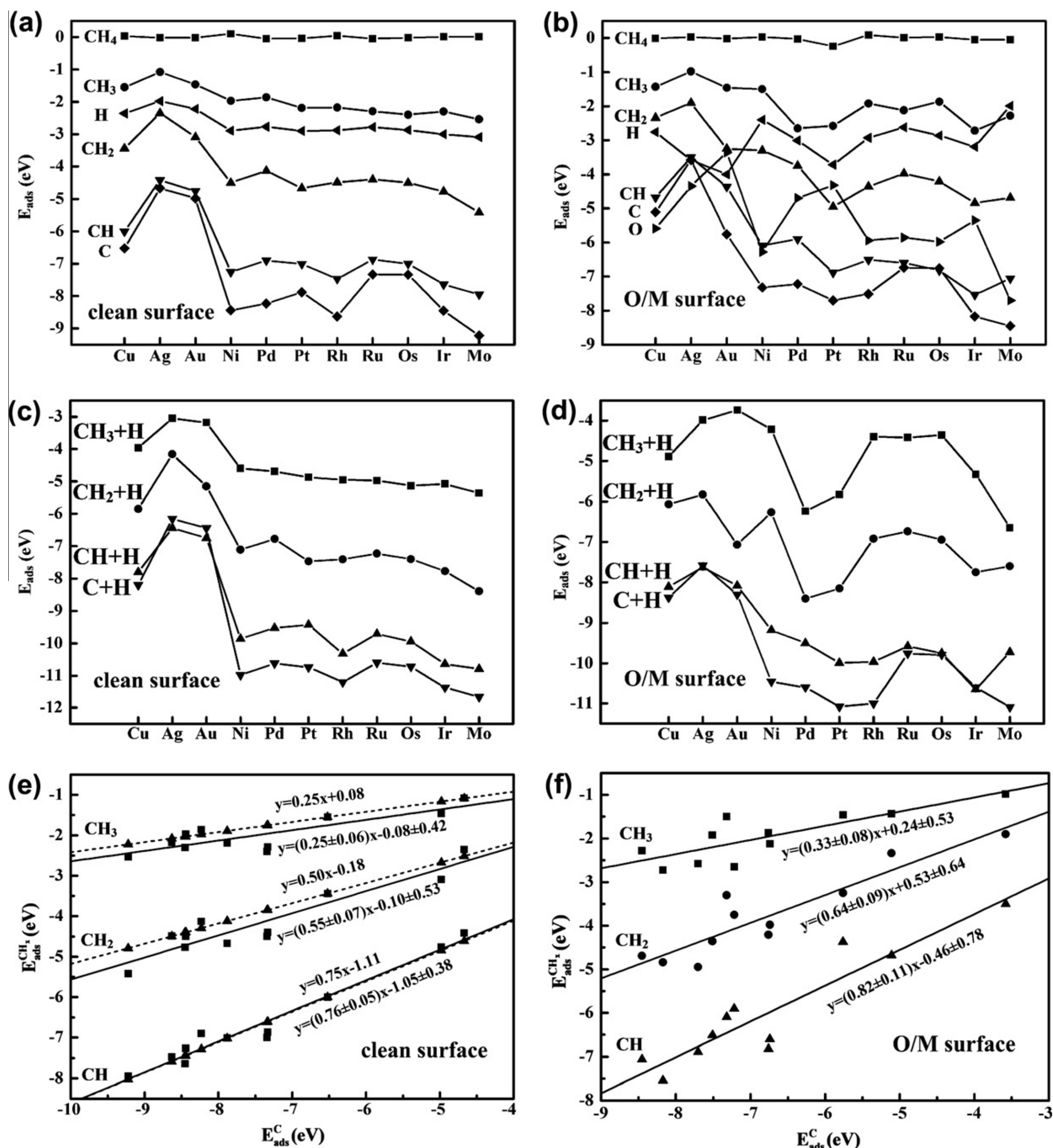

Fig. 1. (a–b) Calculated adsorption energies of CH_x (x = 1–4) species, oxygen atom and hydrogen atom on M(1 0 0) and O/M(1 0 0) surfaces. (c–d) Calculated co-adsorption energies of CH_x (x = 1–3) + H on M(1 0 0) and O/M(1 0 0) surfaces. Adsorption energies of CH_x (x = 1–3) species plotted against adsorption energies of C atom on clean surface (e) and oxygen covered surface (f). Dash line represents linear correlation according to energy data on Cu, and solid line represents linear correlation about calculated results.

due to its incorrect treat on long-range interaction (i.e., dispersion interaction). To explore such effect on the binding energy, the previous DFT calculation of Henkelman et al. [27] indicated that the adsorption energy of methane on Ir(1 1 1) increased by less than 0.10 eV after the correction of dispersion effect. Since both the CH_3 and H are chemisorbed on the metal surface in the TS, the dispersion effect correction on TS can be ignored. Therefore, one can expect that the dispersion effect has a little effect on the activation energy calculation.

The following three dissociation steps $CH_x \rightarrow CH_{x-1}$ + H (x = 3–1) on the IB group metals are also endothermic process, which correspond to higher activation barrier except the third dissociation step on Cu surface (only 0.70 eV, much lower than that on Ag and Au surface). For the remaining transition metals in the series, the energy profile of CH_x (x = 3–1) dissociation is different from that of CH_4 dissociation, with both reaction heat and activation barrier spanning a wider range. The activation barrier for CH_3 dissociation on Ir surface is 0.10 eV, the lowest among all transition metals being considered. For CH_2 dissociation on Ni, Pd, Os, Mo, the corresponding activation barriers are 0.04, 0.08, 0.10, and 0.20 eV. The activation barrier of CH dissociation on Mo is 0.26 eV, which is lower than on the other transition metals.

3.2.2. CH_4 dissociation on the oxygen pre-adsorbed metal surface

We first examine the adsorption of atomic oxygen on these clean metal surfaces, and then, we investigate the reaction of CH_4 dissociation on O/M surfaces. In previous studies, it is found that atomic oxygen prefers high coordinated sites on the clean me-

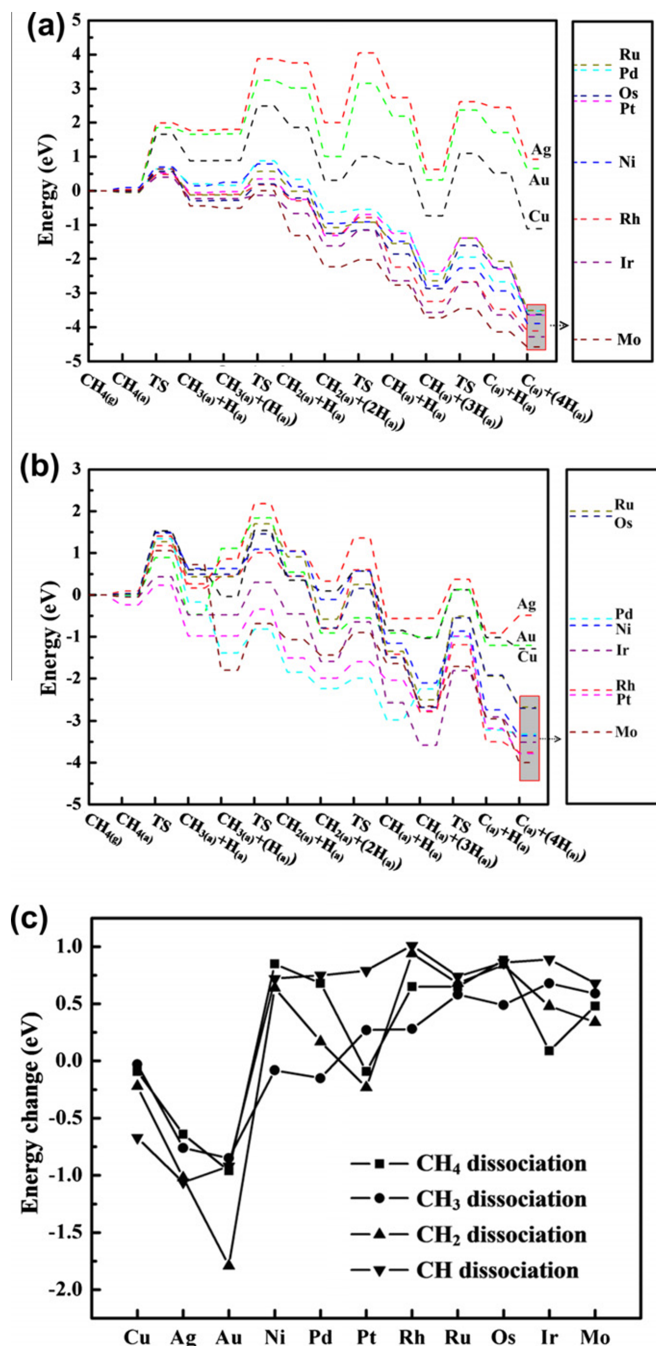

Fig. 2. (a and b) Comparison of CH_4 activation barriers on the transition metal surface with and without pre-adsorbed oxygen atom. (c) Energy change ($E_a^{O/M} - E_a^{clean}$) of different dissociation steps on different metal surfaces.

tal surface [3,18,31]. Hence, the hollow site for oxygen atom has been considered. Results are listed in Table S1, and the order of adsorption energy of atomic oxygen is Au < Pt < Ag < Pd < Ir < Cu < Ru < Rh < Os < Ni < Mo, within a range between −3.36 and −7.70 eV.

For CH_4 dissociation on IB group metal surface, the presence of pre-adsorbed oxygen dramatically decreases the activation barrier of all four dissociation steps. The possible reason is that the C–H bond decomposition mechanism is significantly altered such that CH_4 is activated on IB group metal surfaces, namely the H atom is abstracted by pre-adsorbed atomic oxygen to form hydroxyl. Consider the whole dissociation process on IB group metal surfaces, the promotion effect of the pre-adsorbed oxygen atom is Au > Ag > Cu. On the remaining transition metal surfaces, the CH_4 dissociation process is deactivated by the presence of pre-adsorbed oxygen. The presence of pre-adsorbed atomic oxygen reduces the interaction CH_x-surface, thus reducing the catalytic activity with respect to that of the clean metal surface, particularly, in the CH dissociation case, where activation energy is higher than that for the remaining CH_x species (see Tables S3–S6), probably, the strong adsorption of CH, which means its H atom harder to attract by oxygen than on other adsorbed CH_x groups.

On the clean metal surface, the Brønsted–Evans–Polanyi (BEP) relation [32] is shown for each surface in Fig. 3 a, c, g and i), which is in good agreement with the result calculated by Michaelides et al. [29]. If the value of proportionality parameter in the BEP relationship (α) is small, the TS type is identified as an 'early TS type', whereas $\alpha \approx 1$ relates to a 'late TS type' [33]. For clean metal surfaces, it can be seen from Fig. 3a and Table S7 that transition state energy (E_{TS}) is well correlated with final state energy (E_{FS}) and the slope of the straight line is close to 1, consistent with a 'late TS' for CH_4 activation. For the oxygen pre-covered surface(i.e., O/M surface), the BEP rule failed if the reference system is defined as the oxygen-contained pure slab and reactant in the gas phase. Interestingly, for the O/M surface, if the reference system is defined as pure slab, reactant molecule in gas state and atomic oxygen, and the BEP rule can hold (Fig. 3b, d, f, h and j). This is possibly indication of an 'early TS type' [34].

In this paper, we introduce the idea of activation strain model [35,36], which is helpful for understanding the chemical reactivity of the metal. The activation barriers can be decomposed into the activation strain (ΔE_{strain}, the deformation energy of reactant and substrate) plus the interaction between methane molecule and metal surface (ΔE_{int}). The results for first dissociation step of CH_4 are listed in Table S8. It is found that the activation barrier is determined by the activation strain of CH_4, where the activation strain of substrate is so small that can be neglected and the interaction energy is not large enough to modulate the reactivity trend. On IB group metal surfaces, the strain energy of CH_4 molecule is larger than that on other metal surfaces, which is consistent with higher activation barrier. The dissociation of CH_4 on Ir has the lowest activation barrier of 0.39 eV associated with the smallest deformation energy of CH_4. For the remaining transition metal surfaces, the strain energy basically follows the trend of activation barrier.

3.2.3. Comparison with experimental results

According to the calculated activation barriers on the clean metal surfaces, the most efficient catalyst for CH_4 dissociation is Rh and Ir; Ni, Pd, Pt, Ru, Os, and Mo shows approximately the same catalytic activity; CH_4 dissociation on IB group metals is not favorable. Table S9 listed experimental results about CH_4 activation over different catalyst surfaces. Under different experimental conditions, the conversion rate of CH_4 or the activity of different transition metal both indicate that Ru, Rh, and Ir is better catalyst for CH_4 activation than that on Ni, Pd, and Pt [37–39]. For the IB group metal, activation of CH_4 has a higher activation barrier, 1.04 eV on Cu(1 1 1) [40,41] and 2.54eV on Au cation [42] compared with 0.61 eV on Ni(1 1 1) [40] and Ni(1 0 0) [43]. Many experiments have been performed on the effect of oxygen or the metal in the oxide form on the reactivity of CH_4. From Table S9, it can be found that on Cu(1 0 0) surface, the pre-adsorbed oxygen represents promotion effect [14]. On other transition metal surfaces (Ni, Pd, Ru, and Rh), the metallic site is the active site for CH_4 dissociation [10,40,41,44–46]. Our calculated results is in good agreement with experimental results, that is, the pre-adsorbed atomic oxygen enhanced reactivity of CH_4 on IB group metal surface but inhibits CH_4 dissociation probability on other transition metal surfaces.

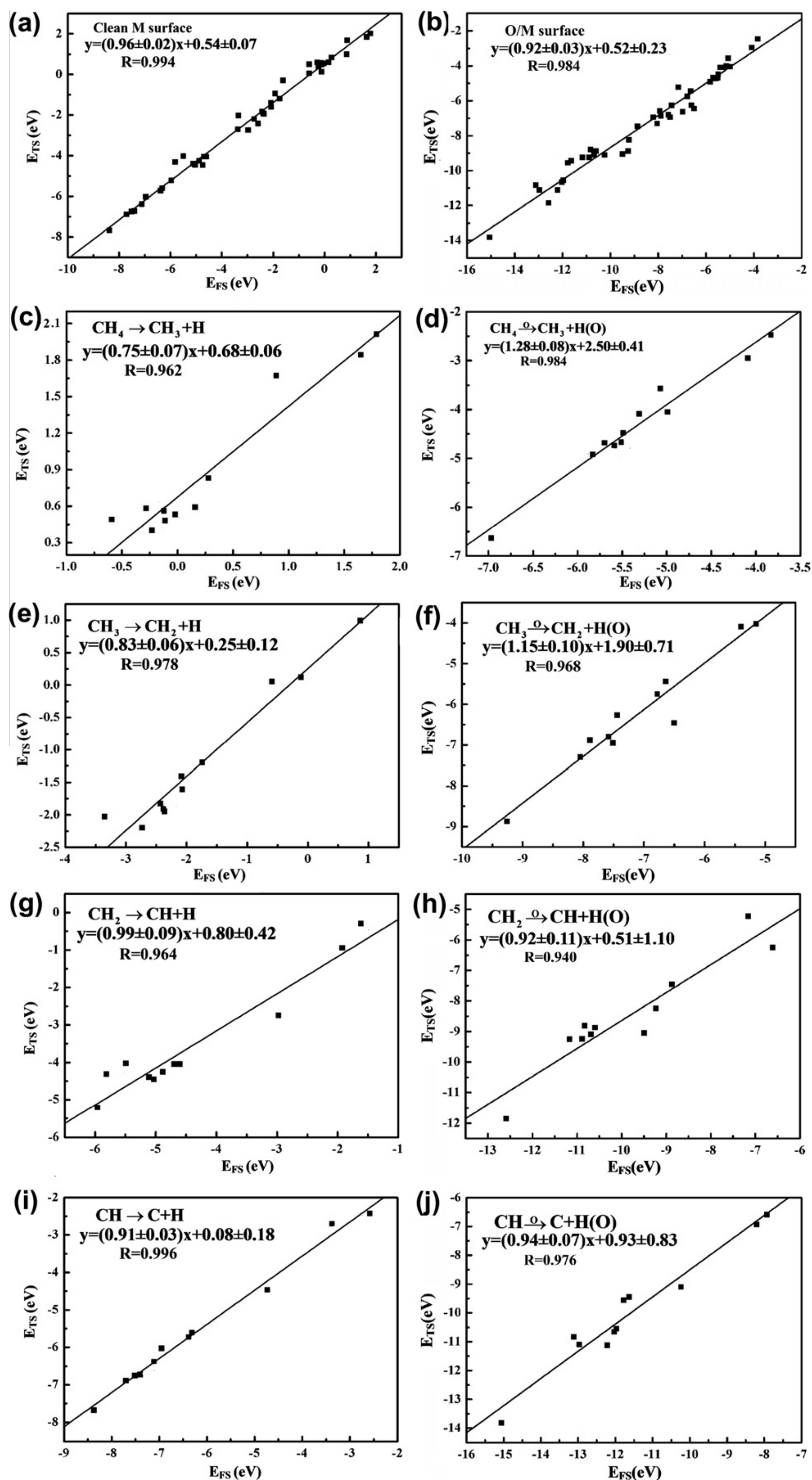

Fig. 3. (a and b) Plots of E_{TS} against E_{FS} for all dissociation steps of CH_4 on M(1 0 0) and O/M(1 0 0) surfaces. (c–j) Plots of E_{TS} against E_{FS} for four individual dissociation steps of CH_4 on M(1 0 0) and O/M(1 0 0) surfaces. E_{TS} and E_{FS} are related to the energy of pure slab, reactant molecule in gas state and atomic oxygen (on O/M(1 0 0) surface).

3.3. Analysis of role of pre-adsorbed oxygen atom in the CH_4 dissociation process

From the calculated results, we find a general rule: The more strongly bound the oxygen atom on the metal surface is, the less the promoting effect or the stronger the inhibiting effect for CH_4 dissociation is. Indeed, a good linear relationship between the atomic oxygen adsorption energy and the activation energy difference ($\Delta E = E_{TS}^{O/M} - E_{TS}^{clean}$) for CH_4 dissociation is found (Fig. 4a–d). This point is close to our previous work about water dissociation on metals [2]. In the following study, we try to gain understanding of the possible reasons behind this phenomenon from both the electronic structure and transition state structures. From the 11 metals studied here, we choose a small subset, namely metallic Au (a less active metal), Cu (a moderate active metal), and Ni (a more active metal).

We calculated the projected density of states (PDOS) localized on O-site at the Fermi level of the pre-adsorbed oxygen system in the IS, in order to explore the reactivity of oxygen atom [47] on Au, Cu, and Ni, previous to studying CH_4 dissociation. Good linear relationships between all possible activation barriers and the Fermi energy PDOS of oxygen 2p orbitals are obtained, which are shown in Fig. 5a. It can be seen that a large Fermi energy PDOS corresponds to the promotion of CH_4 dissociation on metal surfaces by oxygen atom. Since adsorption energy of CH_4 and energy difference for different surfaces are both small, the PDOS onto the CH_4 molecule cannot properly reflect the reactivity change of metal surface with pre-adsorbed atomic oxygen. So, we calculated PDOS onto the CH_3 molecule in the FS for Au, Cu, and Ni (Fig. 5b). It is found that the effect of adsorbed atomic oxygen on PDOS of CH_3 molecule is to shift the HOMO peak closer to the Fermi level on Cu and Au surface, but represents an opposite effect on Ni surface. This is consistent with the promotion effect of pre-adsorbed atomic oxygen for CH_4 dissociation on Cu and Au surface and inhibition effect on Ni surface. The relationship between HOMO energy change of CH_3 molecule and activation energy change is shown in Fig. 5c.

Since the dissociation of CH_4 could produce adsorbed atomic H, it is worth discussing the concept of acid–base pairs in conjunction with our data [34]. In fact, a good linear relationship was found between activation barrier and the adsorption energies of H on these surfaces with pre-adsorbed oxygen atom. As seen in Fig. 5d, one can see that the larger the adsorption energy of H, the weaker the acid is, so the smaller the activation barrier of CH_4 dissociation will be, i.e., the presence of pre-adsorbed oxygen will activates CH_4 dissociation.

The d-band model developed by Hammer and Nørskov [48] was utilized to further explore the role of oxygen atom in the activation of C–H bond. In this paper, we consider the occupied d-band center, which is calculated by the formula: $\varepsilon_d = \frac{\int_{-\infty}^{E_f} E\rho_d(E)dE}{\int_{-\infty}^{E_f} \rho_d(E)dE}$, where ρ_d represents the density of states projected onto metal atom's d-band and E_f is the Fermi energy. In general, the closer to the Fermi energy level of the d-band center, the higher the activity. Fig. 6a displays the PDOS plot of metal atom's d-band for Au, Cu, and Ni surfaces with and without pre-adsorbed oxygen. As seen from Fig. 6, the d-band centers are −3.12, −2.80, −2.40, −2.41, −1.72, and −2.09 eV. This is in good agreement with the activation barrier change, that is, the presence of oxygen promotes the dissociation process on Au, slightly promotes that on Cu, and inhibits that on Ni except the second dissociation step, which is also promoted

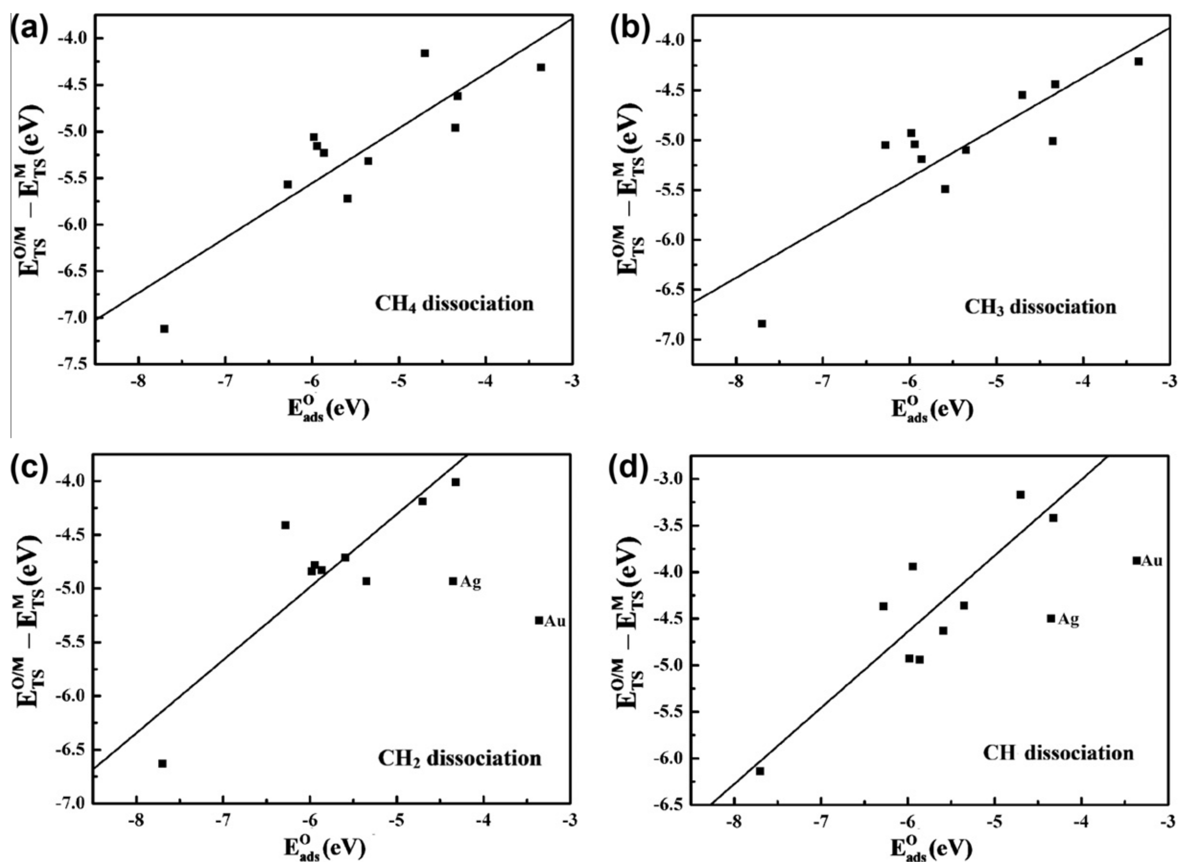

Fig. 4. (a–d) Relationship between activation barrier change of different dissociation steps after oxygen adsorbed on the metal surface and adsorption energy of oxygen atom. (The points with large deviation (Ag, Au in Figs. 4c and 3d) are not included in linear regression.)

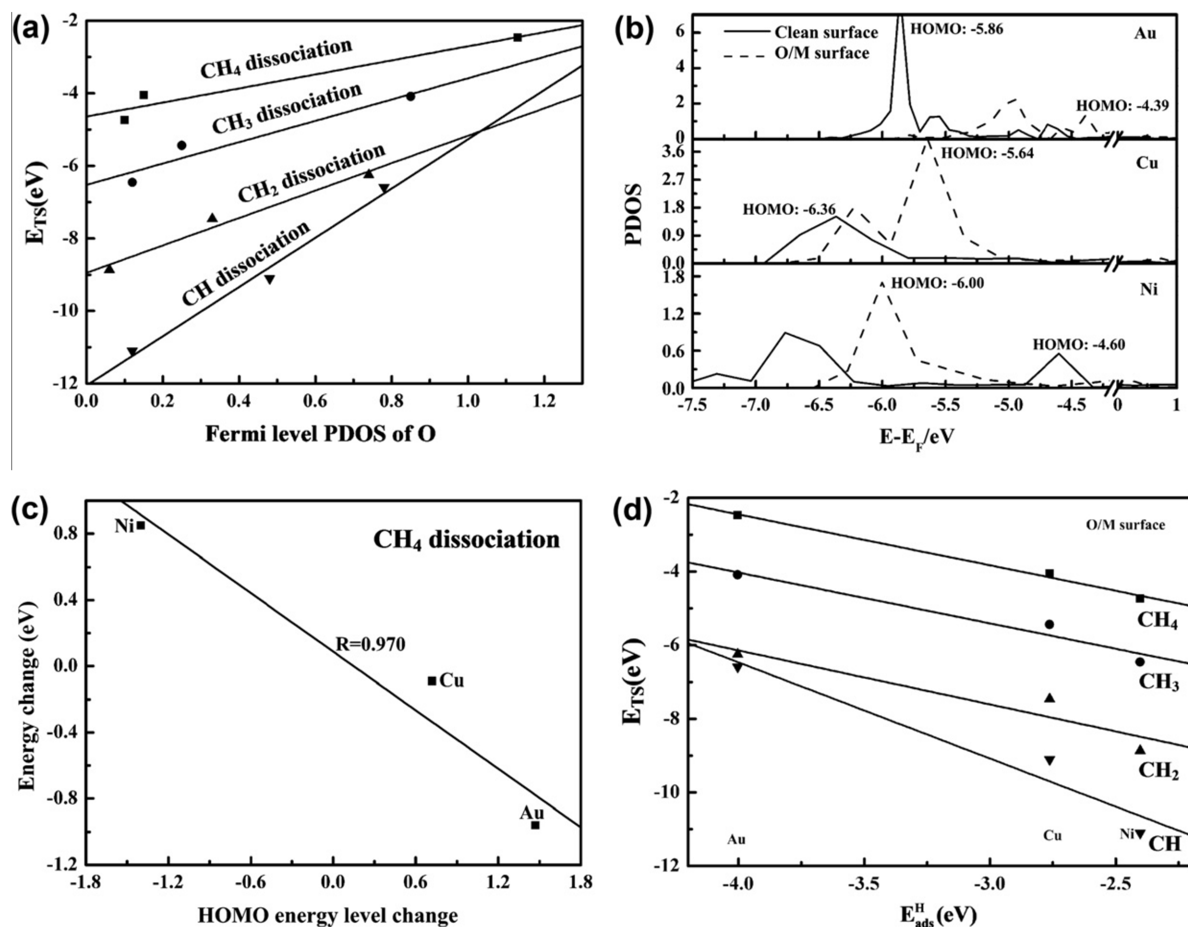

Fig. 5. (a) Relationship between activation barrier and Fermi level PDOS of oxygen. (b) PDOS onto CH_4 molecule in the IS on Au, Cu, and Ni with and without pre-adsorbed oxygen atom. (c) Relationship between energy change and the HOMO energy level change. (d) Plots of E_{TS} against adsorption energies of H atom on O/M surfaces (M = Cu, Au, Ni).

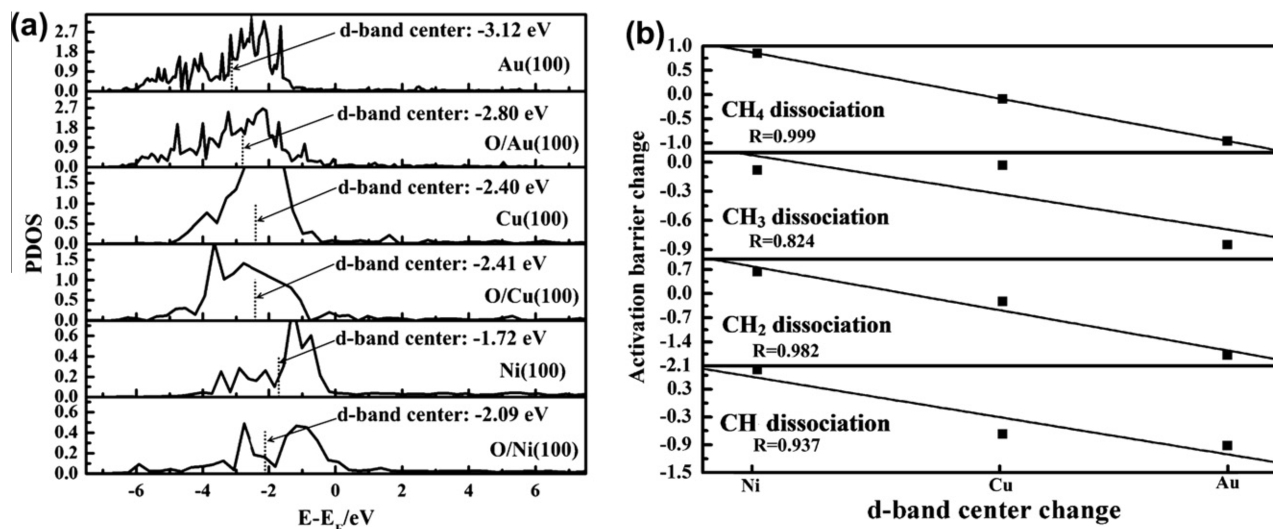

Fig. 6. (a) Projected density of state (PDOS) onto d-band of metal atoms. (b) Relationship between activation barrier change and d-band center change with and without pre-adsorbed oxygen for three dissociation step on Au, Cu, and Ni surfaces.

by the presence of oxygen. Good relationships between the d-band center change and activation barrier change are found for these dissociation steps (shown in Fig. 6). The stabilization energy (E_d) of the metal d-states due to the presence of the TS complex is another method to analyse the reactivity of CH_4 dissociation on different metal surfaces quantitatively [49]. It can be calculated by

Table 1
Energy decomposition of the calculated activation barrier for the first dissociation step of CH_4 on Au(1 0 0), Cu(1 0 0), Ni(1 0 0) with and without pre-adsorbed oxygen atom.

	$E^{IS}_{CH_4}$ (eV)	$E^{TS}_{CH_3}$ (eV)	E^{TS}_{H} (eV)	$\sum E$	E_{int} (eV)	E_a (eV)
Au(1 0 0)	−0.02	−2.07	−1.47	−3.54	0.55	1.87
Cu(1 0 0)	0.03	−2.34	−1.43	−3.77	0.59	1.63
Ni(1 0 0)	0.10	−2.64	−2.03	−4.67	0.53	0.60
O/Au(1 0 0)	−0.02 (0.00)	−2.41 (−0.34)	−0.58 (0.89)	−2.99 (0.55)	−0.96 (−1.51)	0.91
O/Cu(1 0 0)	−0.01 (−0.04)	−2.25 (0.09)	−0.61 (0.82)	−2.86 (0.91)	−0.45 (−1.04)	1.54
O/Ni(1 0 0)	0.03 (−0.07)	−1.81 (0.83)	−1.52 (0.51)	−3.33 (1.34)	−0.03 (−0.56)	1.45

Note: $\sum E = E^{TS}_{CH_3} + E^{TS}_{H}$. Here, the C–H bonding energy of CH_4 (E^{gas}_{bond}) is calculated to be 4.84 eV. The data in the parentheses indicate the different component's contribution (increase or decrease) to the activation barrier compared with the clean metal surface.

the formula: $E_d = \int_{-\infty}^{E_F} \epsilon(n_d^{TS} - n_d^{pure})d\epsilon$, where n_d is the normalized DOS of metal atom with and without the TS complex and ε is the energy level. The calculated E_d is −2.62, −1.71, and −0.03 eV for Au, Cu, and Ni surface, which is consistent with the activation barrier (1.87, 1.63, and 0.60 eV). For O/Au(Cu/Ni) surface, the E_d is −0.41, −2.10, and −1.40 eV corresponding to the activation barrier of 0.91, 1.54, and 1.45 eV. The change of E_d is consistent with the effect of pre-adsorbed atomic oxygen on the CH_4 dissociation, that is, promotion effect for Au and Cu surface and inhibition effect on for Ni surface.

Except for the discussion of the electronic structure effect of the reactant and transition state, it is important to analyze the TS by the energetic decomposition method. The energy decomposition scheme developed by Hammer [50] is a very useful tool to explore the physical nature of energy barrier. The formula is: $E_a = E^{gas}_{bond} - E^{IS}_{CH_4} + E^{TS}_{CH_3} + E^{TS}_{H} + E_{int}$ [51], where E^{gas}_{bond} is the bonding energy of CH_4 in the gas phase, $E^{IS}_{CH_4}$ is the adsorption energy of CH_4 in the IS configuration, $E^{TS}_{CH_3}(E_{H^{TS}})$ is the adsorption energies of CH_3(H) in the TS without H(CH_3), E_{int} is the interaction energy between CH_3 and H in the TS, including the Pauli repulsion [52] between CH_3 and H, which is dependent on the distance between them, and the bonding competition effect [53], which is caused by the nearby atoms. From the energy decomposition results listed in Table 1, it can be found that E_{int} on O/M (here, M = Au, Cu, Ni) surfaces is smaller than that of clean M surfaces. Oxygen is able to reduce the bonding competition between CH_3 and H in the TS via the formation of an O–H bond, and this helps in lower the barrier. On the other hand, pre-adsorbed oxygen weakens the adsorption of CH_3 and H in the TS (except for CH_3 on Au). This is not beneficial for the CH_4 activation, which increases the barrier. The overall result is that the existence of atomic oxygen promotes the dissociation of CH_4 on Au and Cu (the promotion effect is more obvious on Au) but inhibits that on Ni.

4. Conclusions

In this work, CH_4 dissociation on metal surfaces with and without pre-adsorbed oxygen atom is investigated by DFT calculation. From calculated results, it is clearly found that adsorption energies of CH_x groups and co-adsorption energies of CH_x + H increase along with the decrease of the number of H atom in CH_x. The order of catalytic activity of different transition metals for CH_4 dissociation is Ir > Rh > Pt > Os > Ni > Ru > Mo > Pd > Cu > Au > Ag. The presence of pre-adsorbed oxygen promotes CH_4 dissociation on IB group metals (Cu, Ag, Au), but shows the opposite effect to that on transition metals (Ir–Pd). A good BEP relationship for CH_4 dissociation on clean and O/M surfaces is found, which provides a reasonable understanding of the nature of CH_4 dissociation process on different transition metal surfaces. The energy of TS related to gas-phase reactant and activation barrier change is well correlated with the adsorption and local electronic structure properties at the oxygen atom. Moreover, the energy decomposition results explain how the presence of pre-adsorbed atomic oxygen affects the barrier. These findings suggest that the pre-adsorbed oxygen plays an important role in industrial reactions on metal catalysts.

Acknowledgments

This work was supported by the National Natural Science Foundation of China (Grants Nos. 20273034 and 20673063) and the Tianhe-1 supercomputer in Tianjin.

Appendix A. Supplementary material

Supplementary material associated with this article can be found, in the online version, at doi:10.1016/j.jcat.2011.05.027.

References

[1] P.S. Moussounda, M.F. Haroun, B. M'Passi-Mabiala, P. Legare, Surf. Sci. 594 (2005) 231.
[2] G.C. Wang, S.X. Tao, X.H. Bu, J. Catal. 244 (2006) 10.
[3] L.Q. Xue, X.Y. Pang, G.C. Wang, J. Phys. Chem. C 111 (2007) 2223.
[4] E. Shustorovich, A.T. Bell, Surf. Sci. 268 (1992) 397.
[5] C.T. Au, M.W. Roberts, Chem. Phys. Lett. 74 (1980) 472.
[6] B.A. Sexton, A.E. Hughes, N.R. Avery, Surf. Sci. 155 (1985) 366.
[7] B. Afsin, P.R. Davies, A. Pashuski, M.W. Roberts, Surf. Sci. Lett. 259 (1991) L724.
[8] B. Afsin, P.R. Davies, A. Pashusky, M.W. Roberts, D. Vincent, Surf. Sci. Lett. 284 (1993) A280.
[9] A. Boronin, A. Pashusky, M.W. Roberts, Catal. Lett. 16 (1992) 345.
[10] M. Valden, J. Pere, N. Xiang, M. Pessa, Chem. Phys. Lett. 257 (1996) 289.
[11] M.A. Quinlan, B.J. Wood, H. Wise, Chem. Phys. Lett. 118 (1985) 478.
[12] G. Krishnan, H. Wise, Appl. Surf. Sci. 37 (1989) 244.
[13] I. Alstrup, I. Chorkendorff, S. Ullmann, Surf. Sci. 234 (1990) 79.
[14] I. Alstrup, I. Chorkendorff, S. Ullmann, Surf. Sci. 264 (1992) 95.
[15] M. Valden, N. Xiang, J. Pere, M. Pessa, Appl. Surf. Sci. 99 (1996) 83.
[16] F. Besenbacher, J.K. Nørskov, Prog. Surf. Sci. 44 (1993) 5.
[17] C.T. Au, C.F. Ng, M.S. Liao, J. Catal. 185 (1999) 12.
[18] B. Xing, X.Y. Pang, G.C. Wang, Z.F. Shang, J. Mol. Catal. A: Chem. 315 (2010) 187.
[19] G. Kresse, J. Furthmüller, Comp. Mater. Sci. 6 (1996) 15.
[20] G. Kresse, J. Furthmüller, Phys. Rev. B 54 (1996) 11169.
[21] Y. Morikawa, K. Iwata, K. Terakura, Appl. Surf. Sci. 169–170 (2001) 11.
[22] G. Kresse, J. Hafner, Phys. Rev. B 47 (1993) 558.
[23] P.E. Blöchl, Phys. Rev. B 50 (1994) 17953.
[24] G. Kresse, D. Joubert, Phys. Rev. B 59 (1999) 1758.
[25] H.J. Monkhorst, J.D. Pack, Phys. Rev. B 13 (1976) 5188.
[26] F. Abild-Pedersen, J. Greeley, F. Studt, J. Rossmeisl, T.R. Munter, P.G. Moses, E. Skúlason, T. Bligaard, J.K. Nørskov, Phys. Rev. Lett. 99 (2007) 016105.
[27] G. Henkelman, H. Jónsson, Phys. Rev. Lett. 86 (2001) 664.
[28] Z.P. Liu, P. Hu, J. Chem. Phys. 115 (2001) 4977.
[29] A. Michaelides, Z.P. Liu, C.J. Zhang, A. Alavi, D.A. King, P. Hu, J. Am. Chem. Soc. 125 (2003) 3704.
[30] C.Q. Lv, K.C. Ling, G.C. Wang, J. Chem. Phys. 131 (2009) 144704.
[31] X.Y. Pang, L.Q. Xue, G.C. Wang, Langmuir 23 (2007) 4910.
[32] R. Alcalá, M. Mavrikakis, J.A. Dumesic, J. Catal. 218 (2003) 178.
[33] R.A. van Santen, M. Neurock, S.G. Shetty, Chem. Rev. 110 (2010) 2005.
[34] H.-Y. Li, Y.-L. Guo, Y. Guo, G.-Z. Lu, P. Hu, J. Chem. Phys. 128 (2008) 051101.
[35] F.M. Bickelhaupt, J. Comput. Chem. 20 (1999) 114.
[36] W.J. van Zeist, F.M. Bickelhaupt, Org. Biomol. Chem. 8 (2010) 3118.
[37] P.M. Torniainen, X. Chu, L.D. Schmidt, J. Catal. 146 (1994) 1.
[38] D. Qin, J. Lapszewicz, Catal. Today 21 (1994) 551.
[39] J.R. Rostrupnielsen, J.H.B. Hansen, J. Catal. 144 (1993) 38.
[40] C.T. Au, Y.H. Hu, H.L. Wan, Catal. Lett. 36 (1996) 159.

[41] C.T. Au, H.Y. Wang, H.L. Wan, J. Catal. 158 (1996) 343.
[42] F.X. Li, P.B. Armentrout, J. Chem. Phys. 125 (2006) 133114.
[43] B.O. Nielsen, A.C. Luntz, P.M. Holmblad, I. Chorkendorff, Catal. Lett. 32 (1995) 15.
[44] Y. Hu, E. Ruckenstein, Catal. Lett. 57 (1999) 167.
[45] O.V. Buyevskaya, K. Walter, D. Wolf, M. Baerns, Catal. Lett. 38 (1996) 81.
[46] C. Elmasides, D.I. Kondarides, S.G. Neophytides, X.E. Verykios, J. Catal. 198 (2001) 195.
[47] P.J. Feibelman, D.R. Hamann, Phys. Rev. Lett. 52 (1984) 61.
[48] B. Hammer, J.K. Nørskov, Surf. Sci. 343 (1995) 211.
[49] H.F. Wang, Z.P. Liu, J. Am. Chem. Soc. 130 (2008) 10996.
[50] B. Hammer, Surf. Sci. 459 (2000) 323.
[51] G. Fratesi, S. de Gironcoli, J. Chem. Phys. 125 (2006) 044701.
[52] J.J. Mortensen, B. Hammer, J.K. Nørskov, Surf. Sci. 414 (1998) 315.
[53] A. Alavi, P. Hu, T. Deutsch, P.L. Silvestrelli, J. Hutter, Phys. Rev. Lett. 80 (1998) 3650.